Supplement of Earth Syst. Sci. Data, 17, 6315–6330, 2025
https://doi.org/10.5194/essd-17-6315-2025-supplement

Supplement of

A 30 m resolution dataset of soil and water conservation terraces across China for 2000, 2010, and 2020

Enwei Zhang et al.

Correspondence to: Xingwu Duan (xwduan@ynu.edu.cn)

Supplementary materials

Note S1. CSLE model to assess soil erosion

The Chinese Soil Loss Equation (CSLE) is used to assess the soil erosion modulus of cropland in China in 2020. The formula for the CSLE is Eq. (S1) (Liu et al., 2020).

$$A = R \cdot K \cdot L \cdot S \cdot B \cdot E \cdot T \tag{S1}$$

Where *A* is soil loss (t/(hm^2·yr)). *R* is rainfall erosivity (MJ·mm/(hm^2·h·yr)). *K* is soil erodibility (t·hm^2·h/(hm^2·MJ·mm)). *L* is the dimensionless slope length factor. *S* is the dimensionless slope steepness factor. *B* is the dimensionless vegetation cover and biological practice factor. *E* is the dimensionless soil and water conservation engineering practices factor. *T* is the dimensionless tillage and management factor.

Calculation of *R-factor*. Daily rainfall data from 2,417 meteorological stations across mainland China, covering the period from 1991 to 2020, were used to calculate the average annual rainfall erosivity. The calculated values from meteorological stations were interpolated into raster layers with the ordinary kriging method. The rainfall erosivity was calculated using the modified algorithm by Xie et al. (2016), which is as follows:

$$\bar{R} = \sum_{k=1}^{24} \bar{R}_{hmk} \tag{S2}$$

$$\bar{R}_{hmk} = \frac{1}{n} \sum_{i=1}^{n} \sum_{j=0}^{m} \left(\alpha \cdot p_{i,j,k}^{1.7265}\right) \tag{S3}$$

$$\overline{WR}_{hmk} = \frac{\bar{R}_{hmk}}{\bar{R}} \tag{S4}$$

where $\bar{R}$ is average annual rainfall erosivity (MJ·mm/(hm^2·h·yr)), k represents the sequence of half-months in each year, $\bar{R}_{hmk}$ is the rainfall erosivity of the k-th half month within each year (MJ·mm/(hm^2·h·yr)), *n* is the number of years (from 1991 to 2020), *j* is the days of daily erosive rainfall within each half month. The daily erosive rainfall is defined as daily rainfall that is greater than or equal to 12 mm (Xie et al., 2002). The α was set to 0.3957 for warm months from May to September and 0.3103 in remaining months. $\overline{WR}_{hmk}$ is the proportion of the rainfall erosivity in the k-th half month to the average annual rainfall erosivity. Daily precipitation data from approximately 2,400 meteorological stations for the period 1991–2020 were used to calculate the annual average rainfall erosivity. Then, this data was interpolated using ordinary kriging to generate a 250-meter resolution rainfall erosion potential raster layer. The daily precipitation data were obtained from the CAS Resource and Environmental Science Data Platform (https://www.resdc.cn/data.aspx?DATAID=230).

Calculation of *K-factor*. The K-factor at 30 m resolution was obtained from the Center for Geodata and Analysis, Faculty of Geographical Science, Beijing Normal University (https://gda.bnu.edu.cn). To standardize the data resolution, the 30-meter resolution K-factor layer was resampled to 250-meter resolution.

Calculation of *LS-factor*. The LS-factor includes the L-factor and the S-factor, which were calculated based on NASADEM data with 30 m resolution. The NASADEM data can be accessed at the Land Processes Distributed Active Archive Center (https://lpdaac.usgs.gov/products/nasadem_hgtv001/). The S-factor was calculated using segmented calculations for slope less than or equal to 10° based on the method proposed by Wischmeier and Smith (1978), and for slope greater than 10° using the method proposed by Liu et al. (1994).

$$S = \begin{cases} 10.8 sin\theta + 0.03 & \theta \leq 5° \\ 16.8 sin\theta - 0.50 & 5° < \theta \leq 10° \\ 21.9 sin\theta - 0.96 & \theta > 10° \end{cases} \tag{S5}$$

The L-factor was calculated according to the algorithm developed by Foster and Wischmeier (1974).

$$L_i = \frac{\lambda_{out}^{m+1} - \lambda_{in}^{m-1}}{(\lambda_{out} - \lambda_{in}) \times 22.13^m} \tag{S6}$$

where L_i is the slope length factor, λ_{out} and λ_{in} slope length for segment *i* and segment *i-1* in m, respectively. The slope length index (m) was calculated using the modified algorithm proposed by Liu et al. (2000).

$$m = \begin{cases} 0.2 & \theta \leq 1° \\ 0.3 & 1° < \theta \leq 3° \\ 0.4 & 3° < \theta \leq 5° \\ 0.5 & \theta > 5° \end{cases} \tag{S7}$$

To standardize the data resolution, the 30-meter resolution LS-factor layer was resampled to 250-meter resolution.

Calculation of *B-factor*. The B-factor for cropland was set to 1 (Liu et al., 2020). Cropland data were obtained from the 2020 GlobeLand30 dataset. To standardize data resolution, the 30-meter resolution B-factor raster layer was resampled to 250-meter resolution.

Calculation of *T-factor*. The T-factor was calculated based on the China crop rotation map (Liu and Han, 1987). China was divided into three zones, with 12 primary subzones and 38 secondary subzones. Each cropping area zone assigned a specific T factor value (Soil and Water Conservation Monitoring

Center and Ministry of Water Resources, 2018). Then, the vector T was transformed into grid maps with 250 m resolution using GIS software.

Note S2. Calculation of soil erosion area

The soil loss tolerance in different erosion type zones is different. Based on the soil loss tolerance established by the standards for classification and gradation of soil erosion (Ministry of Water Resources of the People's Republic of China, 2008) (Table S13), the soil erosion area for each region is calculated individually. Finally, the erosion area of cropland is aggregated to derive the total erosion area.

Note S3. Calculation of the impact of terraces on soil erosion.

The impact of terraces on soil erosion was evaluated by the differences between scenarios with and without terraces. The calculation method is as follows:

$$SE = (R \cdot K \cdot L \cdot S \cdot B \cdot E \cdot T) - (R \cdot K \cdot L \cdot S \cdot B \cdot T) \quad \text{(S8)}$$

where *SE* represents the soil erosion modulus reduced by terraces.

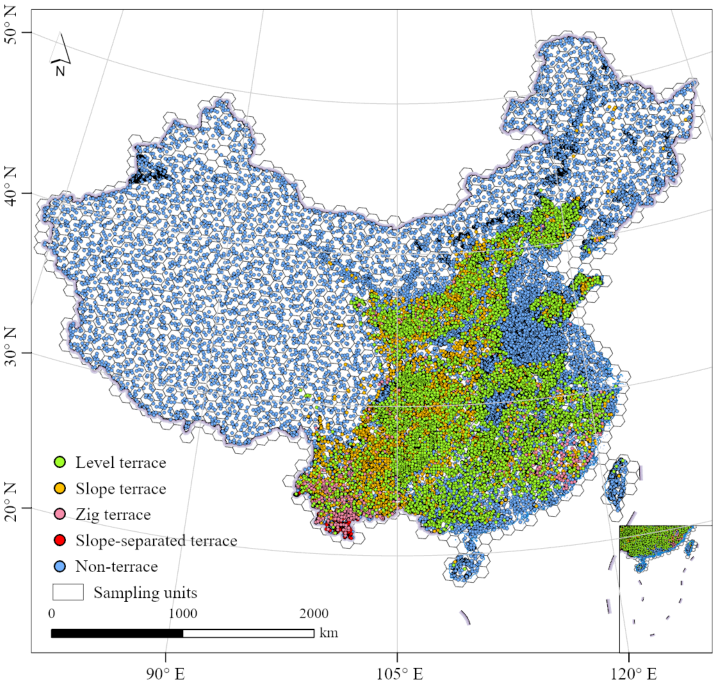

Figure S1. The spatial distribution of train samples in 2020.

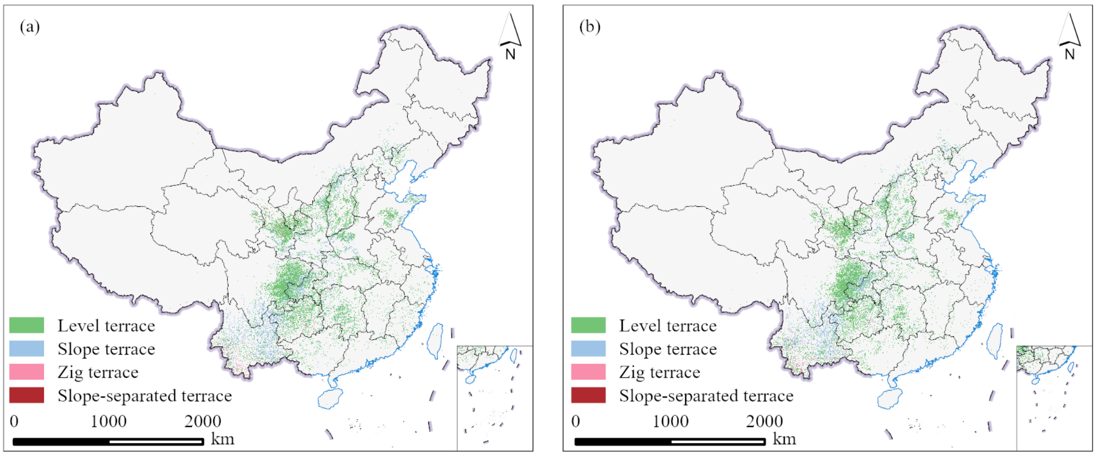

Figure S2. The spatial distribution of terraces from 2000 to 2010. (a) The spatial distribution of terraces in 2000. (b) The spatial distribution of terraces in 2010.

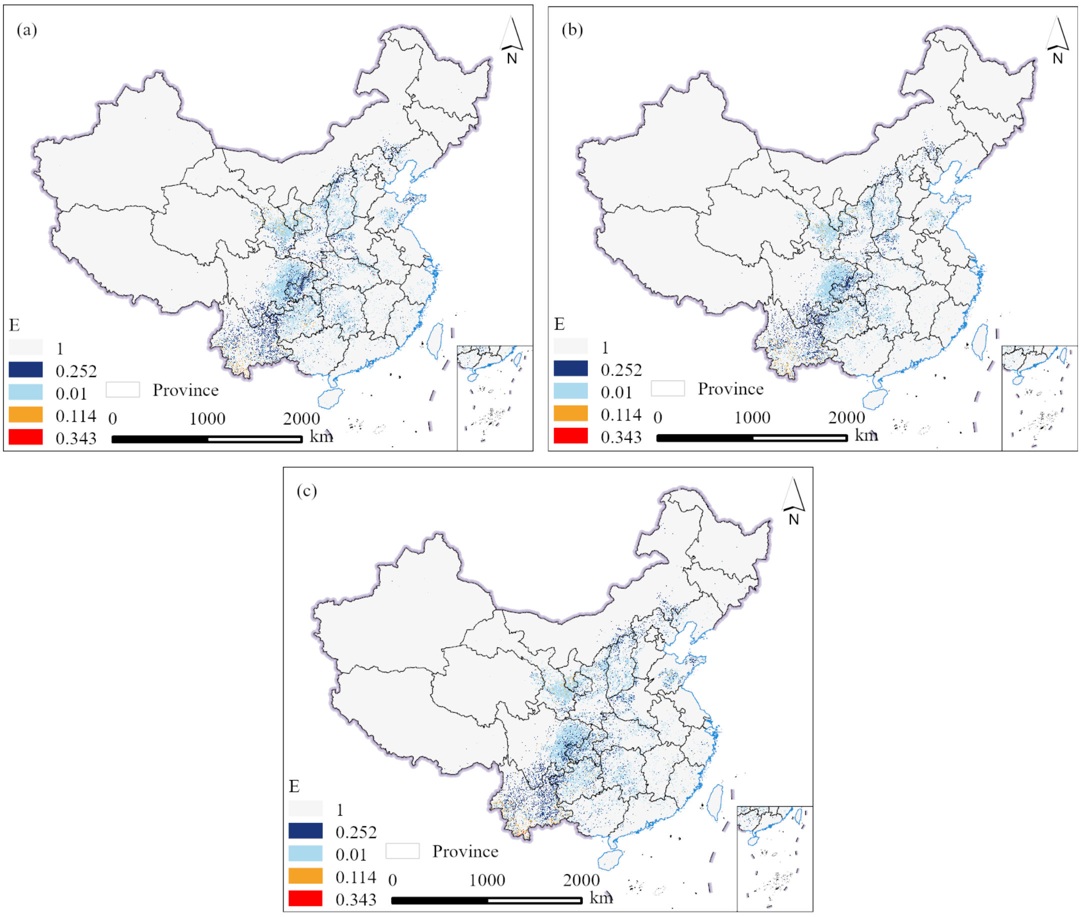

Figure S3. Spatial variances of the value of E. (a-c) Spatial variation of E value in 2000, 2010, and 2020, respectively.

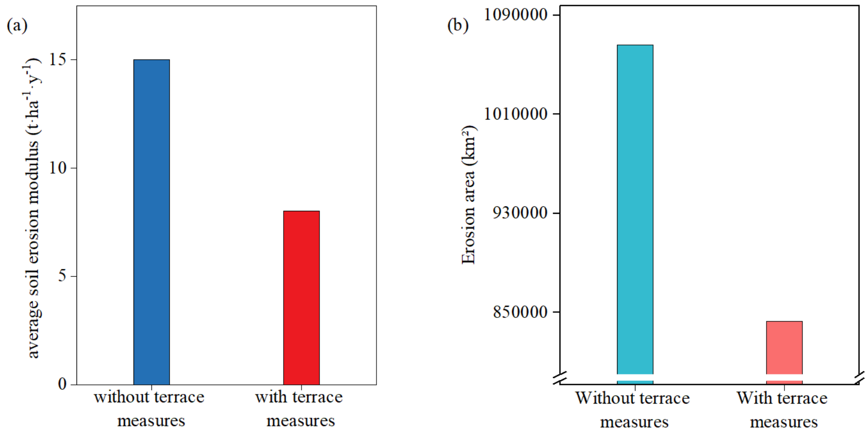

Figure S4. Comparison of soil erosion modulus and soil erosion areas in different scenarios. (a) Comparison of soil erosion modulus with and without terrace measures. (b) Comparison of soil erosion areas with and without terrace measures.

Table S1. The multitemporal data series used in this study.

Data name	Year	Spatial resolution (m)	Data sources
Landsat-5/8 surface reflectance (SR) data	2000, 2010, 2020	30	The data is accessible via GEE and is provided by the United States Geological Survey (USGS) (https://earthengine.google.com/).
Copernicus DEM	2010	30	The data is accessible via GEE (https://earthengine.google.com/).
GlobeLand30	2000, 2010, 2020	30	The data is provided by the National Geomatics Center of China (NGCC) (http://www.globallandcover.com/).

Table S2. Calculation method for feature variables.

Category	Feature	Description	Data source
Spectrum	25th, 50th, and 75th percent quantiles of Landsat SR bands (red, green, blue, near-infrared, shortwave infrared 1, and shortwave infrared 2)	Spectral bands of Landsat SR	Landsat
Spectral indices	25th, 50th, and 75th percent quantiles of NDVI, MNDWI, NDBI, BSI, LSWI, EVI	Normalized indices derived from Landsat SR spectral bands are calculated as: $\mathrm{NDVI} = \frac{(\mathrm{NIR} - \mathrm{Red})}{(\mathrm{NIR} + \mathrm{Red})}$ $\mathrm{MNDWI} = \frac{(\mathrm{Green} - \mathrm{SWIR1})}{(\mathrm{Green} + \mathrm{SWIR1})}$ $\mathrm{NDBI} = \frac{(\mathrm{SWIR1} - \mathrm{NIR})}{(\mathrm{SWIR1} + \mathrm{NIR})}$ $\mathrm{BSI} = \frac{((\mathrm{SWIR1} + \mathrm{Red}) - (\mathrm{Blue} + \mathrm{NIR}))}{((\mathrm{SWIR1} + \mathrm{Red}) + (\mathrm{Blue} + \mathrm{NIR}))}$ $\mathrm{LSWI} = \frac{(\mathrm{NIR} - \mathrm{SWIR1})}{(\mathrm{NIR} + \mathrm{SWIR1})}$ $\mathrm{EVI} = \frac{2.5 * (\mathrm{NIR} - \mathrm{Red})}{(\mathrm{NIR} + 6 * \mathrm{Red} - 7.5 * \mathrm{Blue} + 1)}$	Landsat
Topography	Elevation, slope, aspect, Slope of slope, roughness, slope shape, relief	Topographic feature derived from DEM data are calculated as: Elevation, aspect and slope were calculated using the built-in terrain functions available on the GEE platform. The calculation method methods for Slope of Slope, Roughness, Slope Shape, and Relief were derived from the Digital Elevation Model Tutorial (Tang et al., 2016). $\text{Slope of slope} = \frac{\text{Slope change}}{\text{Horizontal distance change}}$ Slope of Slope was calculated by applying the built-in slope function in GEE to the slope raster layer. $\text{Roughness} = \frac{\text{Curved surface area}}{\text{Plan surface area}}$	Copernicus DEM

Category	Feature	Description	Data source
		When using a 3 × 3 analysis window, Roughness can be calculated using the formula R=1/cos(S), where S represents the slope. $\text{Slope Shape} = H_{i,j} - \frac{\sum_{i=1}^{n} H_i}{n}$ Here, n represents the total number of pixels within the analysis window; $H_{i,j}$ is the elevation value at the center of the analysis window; and H_i is the elevation of the *i-th* pixel within the window. $\text{Relief} = \mathrm{H}_{\max} - \mathrm{H}_{\min}$ H_{max} represents the maximum elevation value within the analysis window, and H_{min} represents the minimum elevation value within the window.	

Table S3. Used features of multi-temporal metrics in 2000 for SWCTMD mapping.

Region	Features for classifying terrace	Features for classifying various terrace types
Southwest China	SOS, SR_B1_p75, SR_B4_p50, SR_B7_p25, aspect, elevation, evi_p25, lswi_p25, mndwi_p25, P, slope	SOS, SR_B1_p50, SR_B4_p25, SR_B4_p75, SR_B5_p75, aspect, elevation, lswi_p75, mndwi_p25, ndvi_p50, P, slope
Northwest China	SOS, SR_B1_p25, SR_B1_p75, SR_B4_p25, SR_B7_p75, aspect, bsi_p25, elevation, evi_p25, lswi_p25, mndwi_p50, P, slope	SOS, SR_B1_p75, SR_B4_p75, aspect, elevation, evi_p25, lswi_p25, lswi_p75, mndwi_p25, mndwi_p75, P, slope
Northeast and North China	SOS, SR_B1_p25, SR_B1_p50, SR_B4_p25, SR_B4_p50, SR_B4_p75, aspect, bsi_p25, elevation, evi_p25, evi_p50, evi_p75, lswi_p25, mndwi_p25, mndwi_p50, P, slope	SOS, SR_B1_p50, SR_B4_p75, SR_B7_p25, aspect, bsi_p25, elevation, evi_p50, evi_p75, lswi_p25, lswi_p50, mndwi_p25, mndwi_p50, mndwi_p75, P, slope
South China	SOS, SR_B1_p25, SR_B1_p75, SR_B4_p25, SR_B4_p75, SR_B7_p25, aspect, elevation, lswi_p25, mndwi_p75, ndvi_p75, P, slope	SOS, SR_B1_p25, SR_B1_p75, SR_B4_p75, SR_B5_p75, aspect, elevation, evi_p25, lswi_p75, mndwi_p25, P, slope
Central China	SOS, SR_B1_p25, SR_B1_p75, SR_B4_p25, SR_B4_p75, aspect, elevation, evi_p50, lswi_p25, lswi_p75, mndwi_p25, P, slope	SOS, SR_B1_p25, SR_B1_p75, SR_B4_p25, SR_B4_p75, SR_B5_p75, aspect, elevation, lswi_p25, lswi_p75, mndwi_p25, mndwi_p75, ndvi_p25, P, slope
East China	SOS, SR_B1_p75, SR_B4_p50, aspect, bsi_p25, elevation, evi_p25, lswi_p25, mndwi_p25, P, slope	SOS, SR_B1_p75, SR_B4_p75, aspect, elevation, evi_p25, lswi_p75, mndwi_p25, mndwi_p75, P, slope

Table S4. Used features of multi-temporal metrics in 2010 for SWCTMD mapping.

Region	Features for classifying terrace	Features for classifying various terrace types
Southwest China	SOS, SR_B1_p75, SR_B4_p75, aspect, elevation, lswi_p75, mndwi_p25, ndvi_p25, P, slope	SOS, SR_B1_p50, SR_B1_p75, SR_B3_p25, SR_B4_p50, SR_B5_p75, aspect, elevation, evi_p25, evi_p75, lswi_p75, mndwi_p25, P, slope
Northwest China	SOS, SR_B1_p25, SR_B1_p75, SR_B4_p25, SR_B4_p75, SR_B7_p25, aspect, bsi_p75, elevation, evi_p25, evi_p75, mndwi_p25, ndvi_p25, P, slope	SOS, SR_B1_p75, SR_B4_p75, aspect, elevation, evi_p25, lswi_p25, lswi_p75, mndwi_p25, mndwi_p75, P, slope
Northeast and North China	SOS, SR_B1_p50, SR_B1_p75, SR_B4_p50, SR_B5_p25, aspect, elevation, evi_p25, evi_p50, lswi_p25, mndwi_p25, P, slope	SOS, SR_B1_p25, SR_B1_p75, SR_B4_p50, aspect, bsi_p25, elevation, evi_p25, evi_p50, lswi_p25, lswi_p50, mndwi_p25, P, slope
South China	SOS, SR_B1_p25, SR_B1_p75, SR_B4_p25, SR_B4_p75, SR_B5_p25, SR_B7_p75, aspect, elevation, lswi_p50, mndwi_p25, ndvi_p25, ndvi_p75, P, slope	SOS, SR_B1_p25, SR_B1_p75, SR_B4_p25, SR_B4_p75, SR_B7_p25, SR_B7_p75, aspect, elevation, lswi_p50, mndwi_p25, mndwi_p75, ndvi_p25, ndvi_p75, P, slope
Central China	SOS, SR_B1_p25, SR_B1_p75, SR_B4_p75, SR_B5_p75, aspect, elevation, lswi_p25, lswi_p75, mndwi_p25, ndvi_p25, ndvi_p75, P, slope	SOS, SR_B1_p75, SR_B4_p25, SR_B4_p75, aspect, elevation, evi_p50, lswi_p25, lswi_p75, mndwi_p25, mndwi_p75, ndvi_p25, ndvi_p75, P, slope
East China	SOS, SR_B1_p75, SR_B4_p50, SR_B7_p25, aspect, elevation, evi_p25, evi_p75, lswi_p25, mndwi_p75, P, slope	SOS, SR_B1_p75, SR_B4_p75, SR_B5_p75, aspect, elevation, evi_p25, mndwi_p25, mndwi_p75, P, slope

Table S5. Used features of multi-temporal metrics in 2020 for SWCTMD mapping.

Region	Features for classifying terrace	Features for classifying various terrace types
Southwest China	SOS, SR_B2_p25, SR_B5_p25, SR_B5_p75, SR_B7_p75, aspect, bsi_p75, elevation, evi_p25, evi_p75, lswi_p25, lswi_p75, mndwi_p25, mndwi_p75, P, slope	SOS, SR_B2_p75, SR_B5_p25, SR_B5_p75, aspect, elevation, lswi_p25, mndwi_p25, ndvi_p75, P, slope
Northwest China	SOS, SR_B2_p50, SR_B5_p25, SR_B5_p75, SR_B7_p25, aspect, bsi_p50, bsi_p75, elevation, evi_p25, evi_p50, evi_p75, lswi_p25, mndwi_p25, ndvi_p25, ndvi_p75, P, slope	SOS, SR_B2_p25, SR_B2_p75, SR_B5_p50, SR_B5_p75, aspect, elevation, evi_p25, lswi_p25, lswi_p75, mndwi_p25, mndwi_p75, P, slope
Northeast and North China	SOS, SR_B2_p50, SR_B5_p25, SR_B5_p75, SR_B7_p25, aspect, bsi_p50, bsi_p75, elevation, evi_p25, evi_p50, evi_p75, mndwi_p25, ndvi_p25, P, slope	SOS, SR_B2_p25, SR_B5_p75, aspect, bsi_p25, elevation, evi_p25, evi_p50, evi_p75, lswi_p25, lswi_p50, mndwi_p25, mndwi_p75, ndvi_p25, P, slope
South China	SOS, SR_B2_p50, SR_B2_p75, SR_B5_p25, SR_B5_p75, SR_B6_p75, aspect, elevation, lswi_p25, lswi_p75, mndwi_p25, P, slope	SOS, SR_B2_p25, SR_B2_p50, SR_B2_p75, SR_B5_p25, SR_B5_p75, SR_B7_p25, aspect, elevation, lswi_p25, mndwi_p25, mndwi_p75, ndvi_p75, P, slope
Central China	SOS, SR_B2_p75, SR_B3_p25, SR_B5_p50, SR_B6_p75, aspect, elevation, evi_p25, lswi_p25, lswi_p75, mndwi_p75, ndvi_p75, P, slope	SOS, SR_B2_p25, SR_B2_p75, SR_B5_p25, SR_B5_p75, aspect, elevation, lswi_p75, mndwi_p25, ndvi_p25, P, slope
East China	SOS, SR_B2_p75, SR_B5_p25, SR_B5_p75, SR_B6_p75, aspect, elevation, evi_p25, lswi_p25, lswi_p75, mndwi_p75, P, slope	SOS, SR_B2_p75, SR_B5_p25, SR_B5_p75, aspect, elevation, lswi_p25, lswi_p75, mndwi_p25, mndwi_p75, P, slope

Table S6. Train samples collected from 2000 to 2010.

Type	2000	2010	2020
Level terrace	9230	8532	8344
Slope terrace	6267	6271	6234
Zig terrace	1159	1228	1248
Slope-separated terrace	301	415	414
Non-terrace	17934	17626	18171
Total	34891	34072	34411

Table S7. Validation samples in 2010.

Non-terrace	**Level terrace**	**Slope terrace**	**Zig terrace**	**Slope-separated terrace**	**Total**
11280	2998	584	104	20	14986

Table S8. Comparison of terrace Areas between SWCTMD in 2020 and CTM2018 Datasets. "Gain" denotes areas identified as terraces only in the SWCTMD dataset, whereas "Loss" refers to areas identified as terraces only in the CTM2018 dataset.

province	CTM2018 (km²)	SWCTMD in 2020 (km²)	Difference (SWCTMD – CTM2018) (km²)	Gain (km²)				Loss (km²)
				Level terrace	Slope terrace	Zig terrace	Slope-separated terrace	Terrace
Anhui	7255.19	5092.39	-2162.80	2414.14	325.61	60.99	/	4963.55
Fujian	9097.75	6637.96	-2459.79	1002.26	510.44	479.38	/	4451.87
Gansu	52248.06	57356.15	5108.09	8007.46	1091.93	339.48	/	4330.79
Guangdong	4982.90	6597.43	1614.52	2051.30	996.20	/	/	1432.97
Guangxi	13133.09	20975.42	7842.33	8423.77	4339.73	/	/	4921.16
Guizhou	46315.57	59035.48	12719.91	9192.84	4410.92	1226.73	6.24	2116.83
Hebei	13751.55	15209.87	1458.32	2853.21	2320.73	/	0.00	3715.62
Henan	14027.56	23705.55	9678.00	7959.63	3491.49	/	17.69	1790.81
Hubei	23267.58	26391.32	3123.74	7600.61	3458.52	/	27.13	7962.52
Hunan	30868.80	40813.88	9945.08	10964.49	5169.61	/	9.15	6198.18
Jiangxi	15564.45	7512.25	-8052.20	2181.49	391.19	296.52	/	10921.41
Ningxia	8035.61	10194.15	2158.53	2247.29	79.69	141.31	/	309.76
Shandong	18302.50	23123.89	4821.39	5771.31	1584.79	46.37	/	2581.08
Shanxi	37062.87	41679.43	4616.57	6286.92	2595.84	0.00	/	4266.19
Shaanxi	30977.01	39467.78	8490.77	7044.01	4313.44	75.73	/	2942.41
Sichuan	83417.53	99285.71	15868.18	13574.22	7424.91	475.86	4.31	5611.11
Yunnan	75073.95	97955.88	22881.93	6853.27	12469.88	7584.56	324.43	4350.22
Zhejiang	6334.11	3807.41	-2526.70	743.45	305.45	94.45	/	3670.05
Chongqing	29746.65	38039.26	8292.62	5864.75	3569.64	479.07	2.59	1623.43
Qinghai	6038.90	6316.37	277.47	792.53	88.16	47.56	0.00	650.78

Table S9. Comparison of terrace Areas between SWCTMD in 2020 and CTM2017 Datasets. “Gain” denotes areas identified as terraces only in the SWCTMD dataset, whereas “Loss” refers to areas identified as terraces only in the CTM2017 dataset.

province	**CTM2017 (km²)**	**SWCTMD in 2020 (km²)**	**Difference (SWCTMD – CTM2017) (km²)**	**Gain (km²)**				**Loss (km²)**
				Level terrace	**Slope terrace**	**Zig terrace**	**Slope-separated terrace**	**Terrace**
Anhui	2320.54	5093.47	2772.93	3935.96	448.74	74.63	/	1686.40
Fujian	6698.71	6636.65	-62.06	2749.31	867.76	686.97	/	4366.09
Gansu	32161.56	57353.72	25192.16	26441.27	4092.22	2106.95	/	7448.28
Guangdong	4208.52	6594.76	2386.24	3697.91	1261.08	/	/	2572.75
Guangxi	7308.95	20976.30	13667.35	12190.39	5446.80	0.00	/	3969.85
Guizhou	25456.48	59035.79	33579.31	27157.62	10924.35	2351.29	11.84	6865.79
Hebei	13537.45	15210.61	1673.16	4921.16	3876.86	/	/	7124.85
Henan	13963.48	23708.82	9745.34	9837.58	4299.97	/	49.04	4441.25
Hubei	14110.44	26391.38	12280.93	13296.29	5157.65	/	41.99	6215.00
Hunan	27467.65	40811.43	13343.79	18362.07	6781.28	/	23.45	11823.01
Jiangxi	9068.41	7510.90	-1557.51	4355.89	581.50	409.47	/	6904.37
Ningxia	3994.61	10195.18	6200.57	6455.23	158.86	755.13	/	1168.64
Shandong	18097.66	23123.08	5025.42	6757.42	2390.43	420.78	/	4543.20
Shanxi	29853.48	41677.98	11824.50	15744.13	5903.42	/	/	9823.05
Shaanxi	28370.55	39467.41	11096.85	14514.39	7367.91	391.46	/	11176.91
Sichuan	59470.14	99284.94	39814.80	36890.96	14167.60	781.83	7.66	12033.25
Yunnan	38251.80	97945.82	59694.02	19271.94	38146.24	13171.54	347.91	11243.60
Zhejiang	2780.66	3807.41	1026.75	2102.36	624.01	202.83	/	1902.45
Chongqing	20357.14	38039.24	17682.10	13703.93	6753.94	688.10	4.21	3468.08
Qinghai	5519.58	6315.62	796.03	1999.26	465.99	281.98	/	1951.19

Table S10. Average accuracy of terrace from 2000 to 2010.

Region	UA (%)	PA (%)	F1 (%)	OA (%)	KA (%)
Central China	77.79	85.15	81.02	87.80	72.10
East China	80.34	68.66	73.80	91.67	68.89
Northeast and North China	61.72	83.50	70.55	94.51	67.63
Northwest China	75.23	91.64	82.32	89.62	75.11
South China	79.17	76.06	77.45	91.32	72.10
Southwest China	89.75	95.81	92.66	90.18	77.90

Table S11. Average accuracy of different terrace types from 2000 to 2010.

Region	Type	UA (%)	PA (%)	F1 (%)	OA (%)	KA (%)
Central China	Level terrace	95.78	94.84	95.31	91.84	71.53
Central China	Slope terrace	68.79	76.06	72.24		
Central China	Slope-separated terrace	85.24	77.02	80.64		
East China	Level terrace	96.45	95.07	95.75	92.42	64.07
East China	Slope terrace	63.74	72.80	67.91		
East China	Zig terrace	63.59	65.88	64.61		
Northeast and North China	Level terrace	93.70	92.87	93.27	89.33	66.50
Northeast and North China	Slope terrace	72.15	74.59	73.21		
Northwest China	Level terrace	94.35	95.87	95.10	91.13	68.07
Northwest China	Slope terrace	65.86	69.37	67.56		
Northwest China	Zig terrace	80.53	65.82	72.36		
South China	Level terrace	92.90	94.06	93.47	89.41	65.34
South China	Slope terrace	74.00	70.00	71.86		
Southwest China	Level terrace	92.23	92.43	92.33	87.50	64.79
Southwest China	Slope terrace	71.14	70.56	70.82		
Southwest China	Zig terrace	71.87	70.47	71.04		

Table S12. Values of E factor.

Level terrace	Slope terrace	Zig terrace	Slope-separated terrace
0.01	0.252	0.114	0.343

Table S13. Soil erosion intensity classification standard.

Level	**Soil erosion modulus ($t{\cdot}ha^{-2}{\cdot}yr^{-1}$)**
Slight (No erosion)	<2, <5, <10
Low	2, 5, 10 ~ 25
Moderate	25 ~ 50
Hight	50 ~ 80
Extremely high	80 ~ 150
Severe	>150

Note: Northwest Loess Plateau < 10, Southern Red Soil Hilly zone/Southwestern Stony Mountain area < 5, Northeast Black Soil zone/Northern Stony Mountain area < 2.

Supplementary references

Foster, G. R. and Wischmeier, W. H.: Evaluating Irregular Slopes for Soil Loss Prediction, Transactions of the ASAE, 17, 305-0309, https://doi.org/10.13031/2013.36846, 1974.

Liu, B., Xie, Y., Li, Z., Liang, Y., Zhang, W., Fu, S., Yin, S., Wei, X., Zhang, K., Wang, Z., Liu, Y., Zhao, Y., and Guo, Q.: The assessment of soil loss by water erosion in China, Int. Soil Water Conserv. Res., 8, 430-439, https://doi.org/10.1016/j.iswcr.2020.07.002, 2020.

Liu, B. Y., Nearing, M. A., and Risse, L. M.: Slope gradient effects on soil loss for steep slopes, Transactions of the ASAE, 37, 1835-1840, https://doi.org/10.13031/2013.28273, 1994.

Liu, B. Y., Nearing, M. A., Shi, P. J., and Jia, Z. W.: Slope Length Effects on Soil Loss for Steep Slopes, Soil Sci. Soc. Am. J., 64, 1759-1763, https://doi.org/10.2136/sssaj2000.6451759x, 2000.

Liu, X. and Han, X.: Zoning of Chinese farming system, Beijing Agricultural University Press, Beijing, 1987.

Ministry of water Resources of the People's Republic of China: Standards for classification and gradation of soil erosion, SL 190-2007, 2008.

Soil and Water Conservation Monitoring Center, Ministry of Water Resources: Technical Regulation for Dynamic Detection of Regional Soil Erosion, 2018.

Tang, G., Li, F., and Liu, X.: Extraction of slope terrain factors, in: Course of digital elevation model, 3rd Edition, Science Press, Beijing, China, 134-156, 2016.

Wischmeier, W. H. and Smith, D. D.: Predicting rainfall erosion losses: a guide to conservation planning, Science and Education Administration, Washington D. C., America, 1978.

Xie, Y., Liu, B., and Nearing, M. A.: Practical thresholds for separating erosive and non–erosive storms, Transactions of the ASAE, 45, 1843-1847, 10.13031/2013.11435, 2002.

Xie, Y., Yin, S., Liu, B., Nearing, M. A., and Zhao, Y.: Models for estimating daily rainfall erosivity in China, J. Hydrol., 535, 547-558, 10.1016/j.jhydrol.2016.02.020, 2016.